



HAL
open science

Multiscale Analysis of Segmental Relaxation in PC/PETg Multilayers: Evidence of Immiscible Nanodroplets

Bidur Rijal, Laurent Delbreilh, Cyrille Sollogoub, Eric Baer, Allisson Saiter

► **To cite this version:**

Bidur Rijal, Laurent Delbreilh, Cyrille Sollogoub, Eric Baer, Allisson Saiter. Multiscale Analysis of Segmental Relaxation in PC/PETg Multilayers: Evidence of Immiscible Nanodroplets. *Macromolecules*, 2022, 55 (15), pp.6562-6572. 10.1021/acs.macromol.2c00691 . hal-04077837

HAL Id: hal-04077837

<https://hal.science/hal-04077837>

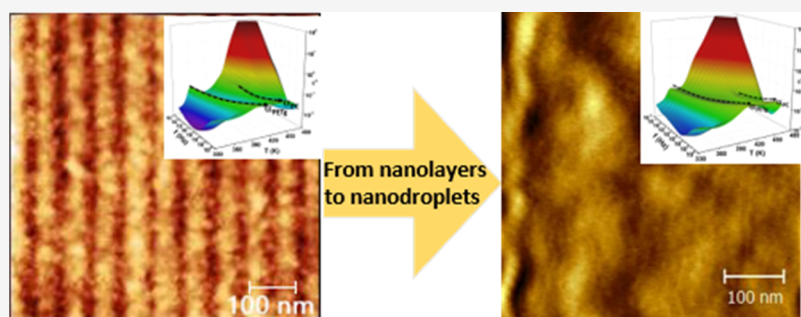
Submitted on 21 Apr 2023

HAL is a multi-disciplinary open access archive for the deposit and dissemination of scientific research documents, whether they are published or not. The documents may come from teaching and research institutions in France or abroad, or from public or private research centers.

L'archive ouverte pluridisciplinaire **HAL**, est destinée au dépôt et à la diffusion de documents scientifiques de niveau recherche, publiés ou non, émanant des établissements d'enseignement et de recherche français ou étrangers, des laboratoires publics ou privés.

Multiscale Analysis of Segmental Relaxation in PC/PETg Multilayers: Evidence of Immiscible Nanodroplets

Bidur Rijal, Laurent Delbreilh,* Cyrille Sollogoub, Eric Baer, and Allisson Saiter-Fourcin



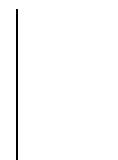
ABSTRACT: This work highlights the influence of layer thicknesses on glass transition and molecular mobility in polycarbonate (PC) and poly(ethylene terephthalate glycol) (PETg) multilayered films obtained by the layer-multiplying coextrusion process. By combining modulated temperature scanning calorimetry (MT-DSC) and dielectric relaxation spectroscopy (DRS) measurements, the average values of the cooperative rearranging region (CRR) size in a wide range of relaxation times and temperatures have been calculated. The size reduction from micro- to nanoscale is accompanied by a significant deviation of the structural and dynamical properties compared to the bulk. Furthermore, we have evidenced significant differences in PETg and PC behaviors: PETg plays the role of a “hard-confined” polymer, while PC behaves as a “free-confined” polymer, implying opposite variations of the glass transition temperature. The determination of the relaxation parameters for each individual polymer has been possible even for very low layer thicknesses (below 10 nm), for which the multilayer structure is not observed. This result shows that even when PETg and PC are brought into very intimate contact, they maintain their own structural behavior and segmental relaxation, suggesting the formation of immiscible nanodroplets when the multilayer structure disappears.

1. INTRODUCTION

Reducing the size of glass-forming materials from micro- to nanoscale is accompanied by a significant deviation of the structural and dynamical properties compared to the bulk.^{1–4} A large number of experiments^{1,5–10} and numerical simulation studies^{11–13} have focused on the variations of the glass transition temperature T_g of polymers with the decrease of thickness. Such variations were observed for the first time for thicknesses smaller than 100 nm and this phenomenon was even amplified for thicknesses below 40 nm.¹⁴ Further, when the size of the system becomes comparable to a characteristic length scale of the system,¹⁵ one may expect to observe some anomalies in the molecular dynamics as a result of the interactions of the system with its boundaries or other finite-size effects.¹⁶ This type of dynamic constraint can be observed when glasses are confined in dimensions close to the cooperative rearranging region (CRR) size (a few nanometers) in porous media,¹⁷ silicate layers,¹⁸ or ultrathin polymer films.¹⁹ Another intrinsic dimension related to molecular mobility is the radius of gyration of the chain:²⁰ When the characteristic dimension of glass reaches this value, T_g may

increase or decrease, depending on the nature of the glassy molecule interactions with the surrounding environment.^{21–23} As explained above, the glass transition of a thin polymer film is not intrinsically associated with the polymer structure itself but reflects its interaction with its surroundings.^{24,25}

During the past decade, numerous studies have been focused on understanding the glass transition phenomena in thin polymer films and the interplay between the substrate and free surface effects. The substantial T_g reduction of around 30 °C, measured using ellipsometry in spin-coated polystyrene (PS) films on silicon wafers, was ascribed to the presence of a liquid-like layer at the free surface of thin films, enhancing the molecular mobility compared to the bulk.¹⁴ A further work from the same group emphasized the role of specific



interactions between the polymer and the substrate in determining the thickness dependence of the T_g of thin films of poly(methyl methacrylate) (PMMA) coated on two different surfaces (gold and silicon oxide substrates).²⁶

As a consequence, the confinement impact on macromolecular mobility strongly depends on the type of confinement: free-standing films, supported thin films, and thin films capped between two surfaces. Compared to these systems, layer-multiplying coextrusion allows the process of films containing thousands of alternating layers, with individual thicknesses that may reach the nanoscale,²⁷ and displaying thin layers symmetrically confined between the walls of another confining polymer. The obtained nanostratified structures have been shown to be relevant to study the impact of nanoconfinement on structural relaxation,^{28,29} the molecular mobility of the amorphous phase, and T_g behavior.^{30–36}

In such systems, the existence of an interdiffusion zone, namely, an interphase, at the interface between the layers of two immiscible polymers must be considered. The interphase thickness may vary depending on the interactions between the two polymers,³⁷ and its impact on the T_g variations and the molecular mobility of the amorphous phase is still an open question. In most multilayered systems, the two glass transition temperatures of the constituent polymers shift closer together as the layer thickness decreases. Such T_g variation is attributed either to an increase of specific interface area and the enhanced diffusion of molecules of one polymer into the other³⁸ or to the confinement effect.³³ For polycarbonate (PC)/poly(methylmethacrylate) (PMMA) multilayered films, Liu et al.^{38,39} observed the merging of “ T_g s” when the individual layer thickness becomes comparable to the interphase dimension (assumed to be around 10 nm), leading to the formation of an interphasic material. Nevertheless, in similar PC/PMMA multilayered systems, two clear distinctive “ T_g s” have been more recently measured using modulated scanning calorimetry for layer thicknesses as thin as 12^{33,34} and 4 nm,³⁰ suggesting that both polymers maintain their integrity. These discrepancies point out the difficulties to determine accurately the effect of nanoconfinement on molecular mobility when two polymers are brought into intimate contact with the formation of an interphase, especially when the layer thickness becomes comparable to the interphase dimension.

The purpose of this work is to investigate another system, composed of amorphous polymers with linear backbones and known to be highly compatible,³⁷ polycarbonate (PC)/poly(ethylene terephthalate glycol) (PETg) multilayered films. In a previous study, Liu et al.³⁷ estimated that the interphase thickness in PC/PETg multilayers was around 30 nm, and they observed, using conventional DSC and DMTA, a single T_g below this thickness. Still, like in the case of the PC/PMMA multilayered systems discussed above, the use of more sensitive and local probes may give new insights into the molecular mixing when the two polymers are brought into very intimate contact, with layer thicknesses typically below 10 nm. In this work, the combination of calorimetric and dielectric fine characterization techniques is used to investigate the influence of layer thickness reduction on dynamic glass transition and molecular mobility. The influence of layer thickness on the cooperativity volume (V_a) and cooperativity degree (N_a) according to Donth’s approach is also discussed.

2. MATERIALS AND METHODS

In the present work, multilayered films comprising alternating layers with different individual thicknesses of PC and PETg were used. PC (grade Makrolon 2207 polycarbonate) with an average molecular weight (M_w) of 30,000 g·mol⁻¹, a monomer unit molar mass m_0 of 254 g·mol⁻¹, and a density ρ of 1.20 g·cm⁻³ was provided by Bayer materials science. PETg (grade Eastar copolyester 6763) used in this study is poly(ethyleneglycol-co-cyclohexane-1,4-dimethanol terephthalate) and was provided by Eastman Chemical Company. It has an average molecular weight (M_w) of 26,000 g·mol⁻¹, a monomer unit molar mass m_0 of 218 g·mol⁻¹, and a density ρ of 1.27 g·cm⁻³. These grades were chosen due to their similar viscoelastic behaviors. Samples were prepared by the multilayer coextrusion technique at the Department of Macromolecular Science and Engineering, CWRU, Cleveland, Ohio, by the research group of Prof. Eric Baer.^{35,38} The technique allows the film fabrication with two or more polymers alternated in thousands of layers. When the layer number in a thin polymer film approaches the thousands, individual layer thicknesses are reduced from micro- to nanoscale. In the present work, films with 33, 257, 1025, and 4097 layers are used, corresponding theoretically to a layer thickness comprised between 1540 and 3 nm (Table 1).

Table 1. Characteristics of the PC/PETg Multilayered Samples Investigated

sample code	number of layers	total film thickness measured (μ m)	theoretical layer thickness (nm)	layer thickness measured (nm)
ML-1540	33	60	1540	1810 \pm 20
ML-200	257	35	200	136 \pm 14
ML-50	1025	50	50	49 \pm 5
ML-25	4097	120	25	29 \pm 3
ML-12	4097	50	12	12 \pm 1
ML-6	4097	40	6	no layer
ML-3	4097	20	3	no layer

The relative composition of each sample is 50:50 (volume) of each polymer. A polarized optical microscopy technique was used to measure the total film thickness of the multilayered samples. For the sake of simplicity, the nomenclature of the sample is ML-X, where ML is for multilayered films and X is for the theoretical layer thickness in nanometers.

Tapping mode atomic force microscopy (TMAFM) was used to characterize the morphology of the multilayered samples having different layer thicknesses. The sample surfaces for AFM imaging were prepared using an ultramicrotome equipped with a diamond knife. For this purpose, a film specimen was embedded in epoxy. Phase and height images were recorded simultaneously.

Modulated temperature scanning calorimetry (MT-DSC) measurements were performed to determine the heat capacity for the multilayer samples. The experiments were performed on a DSC Q100 (TA Instrument). The equipment was calibrated for heat flow, temperature, and baseline (sensor capacitance for Tzero technology) using the standard calibration procedure. The specific heat capacity for each sample was measured using sapphire as a reference. The sample masses were in the range of 4–5 mg, and a modulation amplitude of ± 1 K, an oscillation period of 60 s, and a heating rate of 0.5 K·min⁻¹ were chosen for all of the experiments. These parameters correspond to the “MT-DSC heat cool mode,” allowing the determination of the heat capacity.^{40,41}

The dielectric measurements (frequency range from 10⁻¹ up to 10⁶ Hz) were carried out between 410 and 470 K for the PC bulk, 340 and 410 K for the PETg bulk, and between 333 and 470 K for all of the multilayered samples, in consecutive increasing steps of 1 K. The samples were placed between parallel electrodes, using 30 mm diameter gold plate electrodes. During the whole period of measurement, the sample was kept in a pure nitrogen atmosphere.

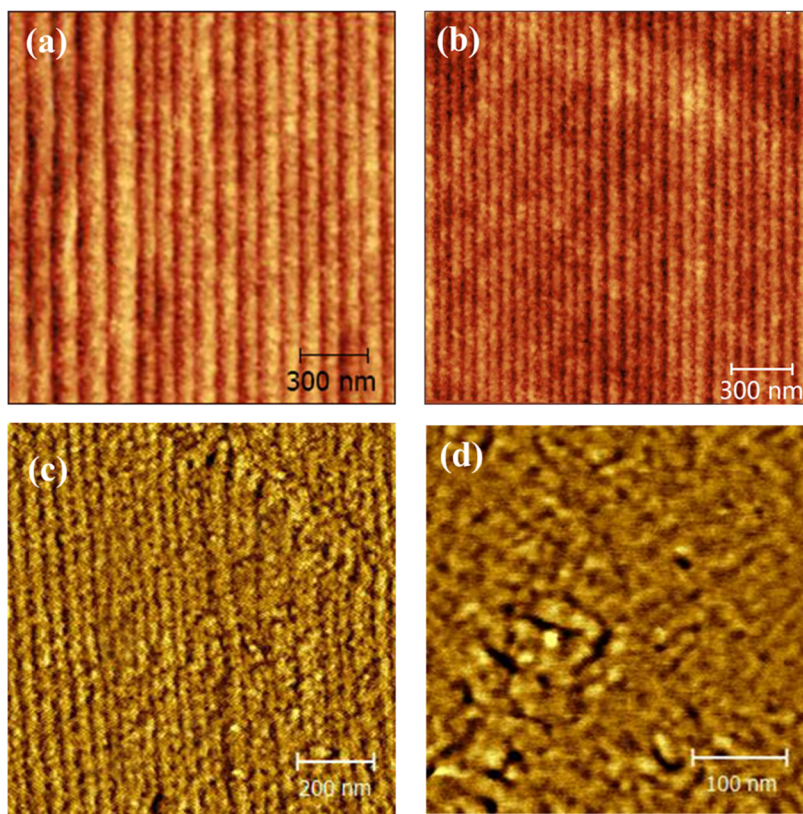


Figure 1. Tapping mode atomic force microscopy height images of PC/PETg multilayered films: (a) ML-50, (b) ML-25, (c) ML-12, and (d) ML-6.

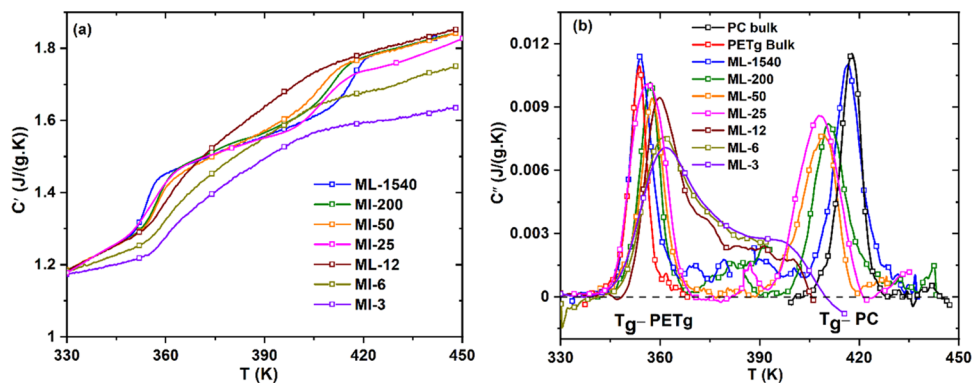


Figure 2. (a) In-phase (C') and (b) out-of-phase (C'') components of the complex heat capacity for different PC/PETg multilayered films presented in [Table 1](#).

The thermal stability of polymer layers during different experimental protocols is a great concern during all studies on multilayered films. To avoid any issues regarding interface stability before each experiment, the films are heated up to a temperature of $T_g + 40$ °C of polycarbonate. Reproducibility is checked in DSC and dielectric relaxation spectroscopy (DRS) experiments, and in a previous paper, this question was addressed, and the AFM picture was taken before and after thermal treatment in a previous study on PC/PMMA films.⁴²

3. RESULTS AND DISCUSSION

3.1. Morphology. The thickness and morphology of the PC/PETg multilayered films were characterized by optical microscopy and AFM, using the procedure developed by Bironeau et al.⁴³ that allows measuring the mean layer thickness with an uncertainty of around 10% by analyzing a

high number of images using an image analysis software. The true total thickness of the films and the thickness of an individual layer were measured and are reported in [Table 1](#).

The average measured thicknesses for different films are in good agreement with the expected theoretical thicknesses. [Figure 1](#) illustrates the AFM height images of the multilayered samples with different layer thicknesses ranging from 50 nm down to 6 nm. A continuous layered structure is observed for individual layer thickness down to 12 nm ([Figure 1b](#), ML-24.8); however, when the layer thickness becomes less than 12 nm, no continuous layers are visible. It seems that below 12 nm, the layers lose their integrity and transform into nanodroplets, as observed in [Figure 1d](#). Similar layer breakups leading to nanodroplets have already been observed^{44–46} and Bironeau et al.⁴⁴ reported the existence of a critical layer

thickness of around 10 nm in PS/PMMA nanolayers, below which the layers break up spontaneously. For PC/PETg systems, as revealed in Figure 1, this critical thickness would be comprised between 6 and 12 nm, which is consistent with what was observed by Bireneau et al.⁴⁴

3.2. Modulated Temperature Differential Scanning Calorimetry (MT-DSC). Figure 2 represents the results obtained from the MT-DSC measurements on the samples. As shown in Figure 2a, for layers thinner than ~ 50 nm (ML-50), the real component of the heat capacity C' does not appear as a step at T_g . For the other samples, two endothermic events associated with their dynamic glass transitions can be observed. From $C'(T)$ curves, the values of the glass transition and the heat capacity step $\Delta C_p(T_g)$ at T_g (recalculated for the real amount of each polymer) are determined. These values are reported in Table 2. It appears that the glass transition

Table 2. Heat Capacity Change at T_g , Glass Transition Temperature T_g , and Fragility Index Values m for the PC/PETg Multilayered Systems

sample	$\Delta C_p(T_g)$ [J/(g·K)]	T_g ($\tau \sim 10$ s) K [MT-DSC]	T_g ($\tau = 100$ s) K [DRS]	fragility [m]
PETg				
bulk	0.28	353.5	349.2	149
ML-1540	0.29	354.0	349.2	150
ML-200	0.28	357.6	352.3	148
ML-50	0.27	357.1	351.0	148
ML-25	0.21	355.2		
ML-12		359.4	356.1	145
ML-6		361.5	355.0	138
ML-3		362.8	356.1	137
PC				
bulk	0.24	418.1	414.3	173
ML-1540	0.25	417.1	412.4	180
ML-200	0.21	410.6	405.9	172
ML-50	0.17	408.2	403.4	173
ML-25	0.12	405.5		
ML-12			400.6	148
ML-6			401.9	140
ML-3			398.4	132

temperatures of PETg [T_g (bulk ≈ 353 K)] and PC [T_g (bulk ≈ 418 K)] remain almost constant for layer thickness in the micrometer range for both components. However, a significant shift of T_g can be observed when the layer thickness decreases below 200 nm (ML-200), toward higher temperatures for PETg and lower temperatures for PC. This opposite effect, already observed in the literature,^{35,36} is attributed either to the presence of an interphase (the proportion of which increases as the number of layers increases) and/or to a change in mobility.

While for the films with layer thickness superior to 12 nm, two distinctive endothermic events are clearly seen, a broadening and asymmetric signal at the glass transition is observed for layer thicknesses thinner than 12 nm, generally interpreted as the signature of interactions between the two polymers that may eventually lead to the interdiffusion of the layers. In our case, it may be related to the loss of layer integrity as observed by AFM images. However, the limit of resolution of both AFM and MT-DSC does not allow to conclude whether the two polymers, below 12 nm, merge or are still present as two distinct phases with the formation of a nanoblend morphology. Further analysis, like dielectric spectroscopy analysis, is needed to conclude on this point.

3.3. Dielectric Spectroscopy Analysis. The three-dimensional (3D) dielectric loss spectra obtained by full temperature and frequency range permittivity measurements carried out with DRS on two multilayered films (ML-50 and ML-6) are presented in Figure 3.

Figure 3 shows that, for a given layer thickness, the segmental relaxation mode can be easily observed on the whole frequency range for PETg and only at high frequencies for PC. Further investigations are needed to analyze low frequencies. Moreover, the two segmental relaxation modes appear for both samples independently of the layer thickness. This point is of particular interest and reveals that even when the layers are not visible, i.e., for multilayered films with layer thicknesses below 12 nm (see the AFM image of ML-6 in Figure 1d), each polymer still has its independent dielectric relaxation ability. This result suggests that even when the two polymers are brought into intimate contact, each polymer exists as an immiscible phase, supporting the idea of the formation of nanodroplets. Similar behavior has previously been observed in studies treating the complex questions of polymer blends. In these papers, the authors, using dynamic mobility tracers in a polymer matrix, observed several unusual behaviors related to the independent relaxation behavior of each polymeric component of the mixture.⁴⁷ Even in miscible polymer blends,

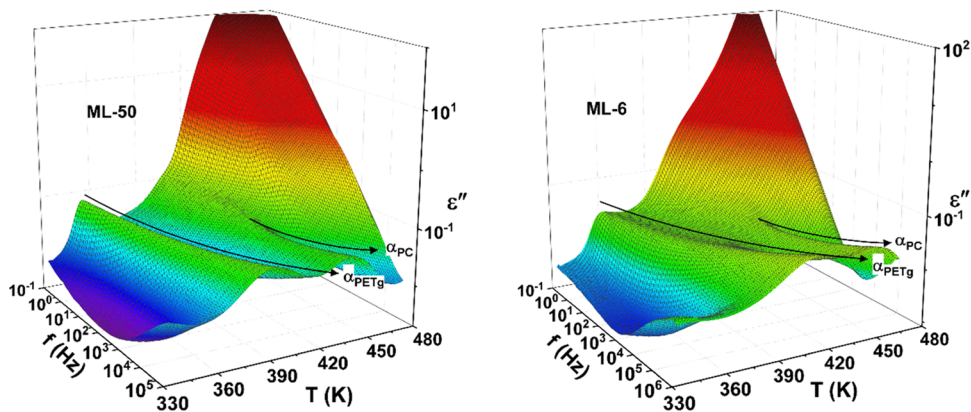


Figure 3. 3D representation of the dielectric loss signal vs temperature and frequency for ML-50 (left) and ML-6 (right).

independent T_g of each component has been evidenced and predicted using the Lodge–McLeish approach.⁴⁸

To analyze and compare the evolution in the temperature/frequency domain spectra of the different multilayered samples, the dielectric response of the multilayers has to be corrected by considering the contribution of each component (described in detail in the Supporting Information). To extract the relaxation times, the complex permittivity signals associated with the α -process for each component were fitted with the empirical Havriliak–Negami (HN) function⁴⁹

$$\varepsilon^*(\omega) = \varepsilon_\infty + \frac{\Delta\varepsilon}{[1 + (i\omega\tau_{\text{HN}})^{\alpha_{\text{HN}}}]^{\beta_{\text{HN}}}} \quad (1)$$

where ε_∞ is the unrelaxed dielectric permittivity, $\Delta\varepsilon$ is the relaxation strength, τ_{HN} is the characteristic relaxation time, and α_{HN} and β_{HN} are shape parameters describing the symmetric and asymmetric broadening factors of the dielectric spectra. The conduction effects were analyzed by adding a contribution to the dielectric loss ε'' : $\sigma_0/[\omega^s\varepsilon_0]$, where σ_0 accounts for the ohmic conduction related to the mobile charge carriers, s is a fitting parameter, and ε_0 is the permittivity of vacuum. Figure 4 shows τ_{max} as a function of

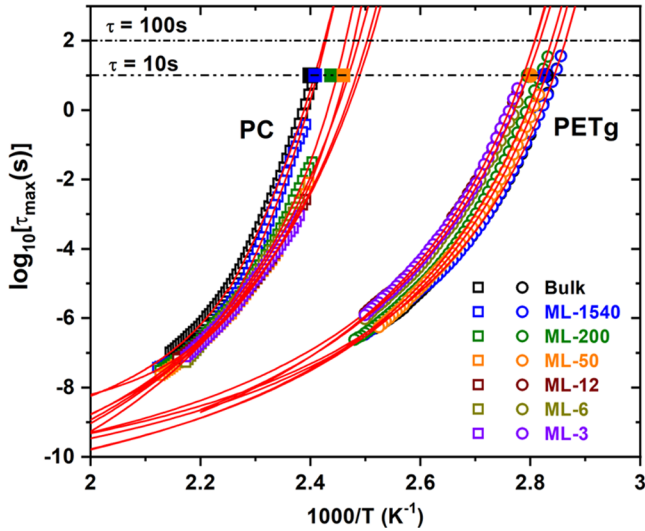


Figure 4. Arrhenius plot of the dielectric relaxation times (τ_{max}) for α -relaxation as a function of the inverse temperature for bulk and multilayered systems. Hollow symbols are from DRS experiments and filled symbols from MT-DSC experiments (period = 60 s, $\tau \sim 10$ s). Solid red lines represent the VFT fits for each sample.

the inverse temperature (Arrhenius diagram) for bulk and multilayered samples. As the layer thickness is reduced from micro- to nanoscale, the α relaxation times for multilayers show some interesting features: a weak but noticeable change in the segmental dynamics of PETg, and a strong increase in the relaxation times on decreasing the layer thickness for PC. For α -relaxation, a non-Arrhenius behavior can be described by the empirical Vogel–Fulcher–Tammann (VFT) equation^{50–52}

$$\tau(T) = \tau_0 \exp\left(\frac{B}{T - T_0}\right) \quad (2)$$

where τ_0 is the relaxation time at infinite temperature, B is a fitting parameter, and T_0 is the so-called Vogel temperature.

The fits are represented by the red lines in Figure 4. The glass transition temperature can be estimated by extrapolating these fits to the common convention, $\tau = 100$ s or $\log_{10}(\tau) = 2$.⁵³ The values of the parameters obtained from the fits are reported in Table 2. To correlate the temperature dependence of the relaxation times to the dynamic glass transition, we have added MT-DSC data at $\tau \sim 10$ s for each sample. The glass transition temperature estimated from MT-DSC is comparable to the values obtained from DRS measurements (Figure 4).

As shown in Table 2, the T_g values extracted from MT-DSC and DRS measurements follow the same tendency as a function of the layer thickness.

Figure 5 shows the thickness dependence of $(T_g - T_{g,\text{bulk}})$ values obtained by these two experimental techniques.

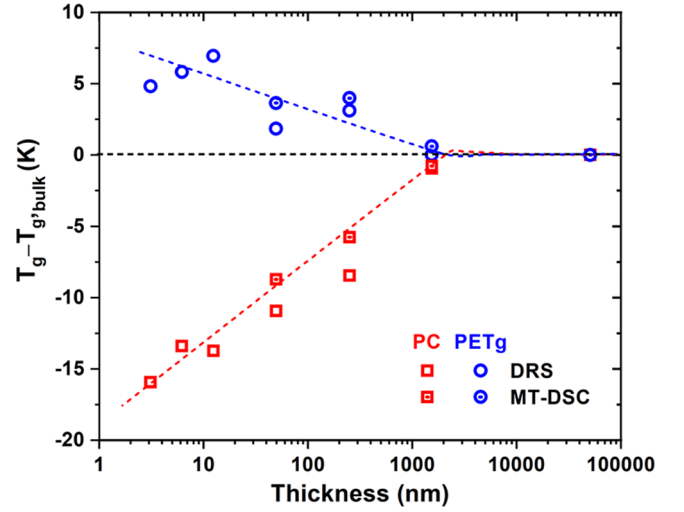


Figure 5. Thickness dependence of $(T_g - T_{g,\text{bulk}})$ for bulk and multilayer systems from DRS and MT-DSC measurements. Dashed curves are guides for the eyes.

Interestingly, when the layer thickness is in the range of micrometer, i.e., the range similar to bulk-like behavior, the glass transition is almost constant. But when the layer thickness decreases from micro- to nanoscale, T_g values diverge from bulk values for PETg and PC systems: a slight increase of T_g for PETg with respect to the bulk, and a huge decrease of T_g for PC with respect to the bulk. These opposite variations of T_g have already been measured on other multilayered systems^{32,33} and have already been observed in different simulation works.⁵⁴ They have been attributed to the creation of strongly confined interfacial zones. We may assume that in our case, below 12 nm layer thickness, the layers tend to lose their integrity and transform into nanodroplets, where the geometrical confinement is even stronger compared to nanolayers, inducing huge variations in the glass transition temperature. A similar evolution of the molecular mobility of the “low- T_g ” component of PC/PMMA multilayer films was measured by Casalini et al.³⁰ They suggested that the presence of PC within the interfacial region significantly increased the T_g of PMMA and slowed down its segmental dynamics. This effect on multilayer systems has also been observed as a function of the type of confinement: Baglay et al.⁵⁵ observed asymmetrical variation of local T_g of PS by depositing in contact polystyrene ($T_{g,\text{bulk}} = 101$ °C) with two different bulk materials, one with higher T_g (180 °C), polysulfone, and another (poly(*n*-butyl methacrylate) (PnBMA)) with $T_g = 21$ °C. In their study, the

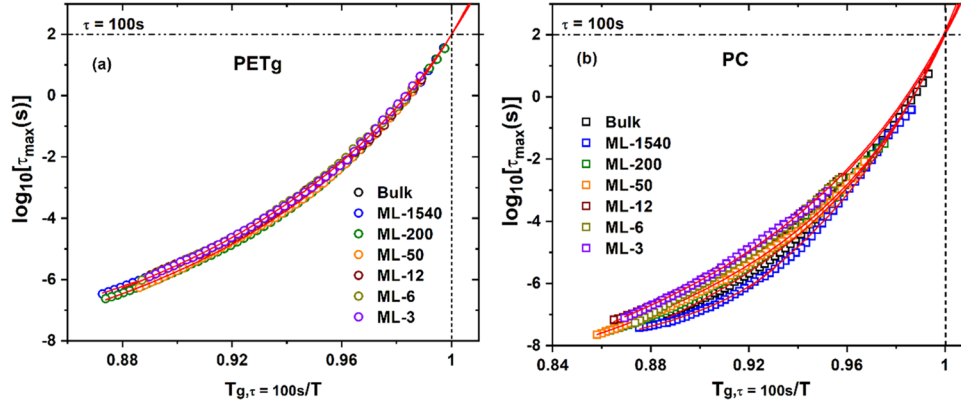


Figure 6. Angell's plot (relaxation time vs T_g/T) of (a) PETg and (b) PC. The red lines represent the VFT fits for each sample. Here, T_g corresponds to $\tau = 100$ s.

authors concluded that the variation of local T_g at the interface is only driven by the type of imposed confinement: hard (PS as the vitreous component at T_g) or soft confinement (PS as the rubbery component at T_g).

A large number of studies can be found on the topic of polymer thin films at the nanometric scale, freely deposited or supported thin films, multilayered thin films, etc. These studies relate the great interest for the understanding of the confinement effect on the glass transition temperature T_g and the fragility index m related to the deviation degree from Arrhenius-type temperature dependence near T_g as proposed by Angell et al.^{56,57} The classification of glass formers in terms of the fragility index allows understanding the slowing down of the molecular mobility along the dynamical glass transition zone. Materials called fragile exhibit markedly non-Arrhenius temperature dependence of the relaxation time close to T_g . The systems called strong exhibit linear temperature dependence of the relaxation time in the Arrhenius diagram. The fragility or steepness index can be quantitatively defined by the following equation^{58,59}

$$m = \left. \frac{d \log_{10} \tau(T)}{d(T_g/T)} \right|_{T=T_g} \quad (3)$$

Using the VFT expression (eq 2), the fragility index m can be calculated according to the following equation

$$m = \frac{BT_g}{(T_g - T_0)^2 (\ln 10)} \quad (4)$$

Evans et al.⁶⁰ and Marvin et al.⁶¹ explained the fragility as a key parameter in determining the strength of the T_g -confinement effect in freely deposited thin films. Polymers that require greater cooperativity in their segmental mobility are expected to experience a greater perturbation to T_g by the presence of a free surface, and these perturbations propagate into the film interior. Fragility is a property that reflects the "relative efficiency of packing complex-shaped molecules".⁶² Polymers with greater packing frustration generally have a larger number of repeat units involved in the cooperative segmental mobility associated with the α -relaxation process. Therefore, higher fragility in the linear polymer may be expected to experience larger T_g confinement effects.⁶³

The temperature dependence of the α relaxation time in a temperature-normalized scale T_g/T (i.e. Angell's plot) is shown

in Figure 6. The fragility index values estimated from eq 4 are reported in Table 2 for different samples.

To better understand the effect of thickness reduction on fragility, the values of the normalized fragility ($m/m_{(bulk)}$) as a function of the layer thickness are presented in Figure 7. It can

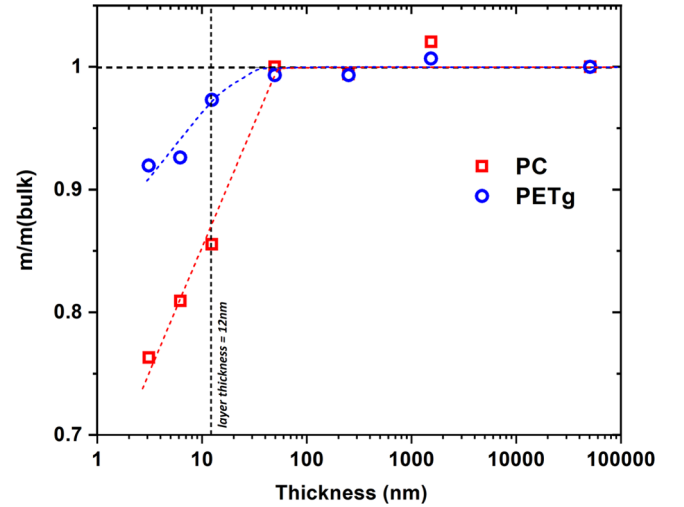


Figure 7. Normalized fragility values ($m/m_{(bulk)}$) as a function of layer thickness for the PC/PETg multilayered films. Dashed lines are guides for the eyes.

be observed that as the layer thickness reduces from micro- to nanoscale, fragility values (see Table 2) decrease for both PC and PETg. More precisely, a small change in the fragility index is observed for PETg, from $m = 150$ down to 137, while a stronger variation is observed for PC, from $m = 172$ down to 132. This huge variation is clearly related to a confinement effect. It can then be assumed that the confining polymer (PC) and the confined polymer (PETg) undergo different conformational modifications as well as the relaxation environment.^{63,64} In a previous study³⁴ on PC/PMMA multilayer films, similar variations of the fragility index for PC with the layer thickness decrease (from $1.64 \mu\text{m}$ down to 12 nm) have been observed. In the case of PMMA, the fragility index remained independent of thickness reduction, which seems to be at the origin of the very weak variations of the glass transition in multilayer geometry. Similar results were also reported by Simon and co-workers^{65,66} on fragility index evolution vs film thickness (from 22 up to 350 nm) of PC. When decreasing the film thickness,

the fragility index also decreases. However, their result for the fragility index of PC bulk ($m = 102$) is lower than generally reported in the literature.^{67,68}

The molecular dynamics in liquids approaching their dynamic glass transition temperature is characterized by cooperativity/or heterogeneity.⁶⁹ This is to say that the correlation between the motions of nearby units (e.g., the monomeric units in the case of polymers) has a strong component associated with causality: a certain number of monomer units may change their positions provided the neighboring ones happen to move concurrently to allow for a sufficient free volume to be accessible. This concept underlies the definition of the cooperatively rearranging region (CRR) in the scheme proposed by Adam and Gibbs⁷⁰ and more recently through the concept of Donth.⁷¹ According to Donth et al.,^{71,72} N_α , the number of relaxing structural units per CRR also called the cooperativity degree, is estimated using the following relation

$$N_\alpha = \frac{N_A k_B T_\alpha^2 \Delta C_p^{-1}}{m_0 (\delta T)^2} \quad (5)$$

where ΔC_p^{-1} is the difference in the inverse of the isobaric heat capacity between the liquid and the glass at T_α (for details, see ref 72), T_α is the dynamic glass transition temperature, k_B is the Boltzmann constant, N_A is the Avogadro's number, m_0 is the molar mass of the relaxing structural unit, and δT is the temperature fluctuation in the CRR.

This approach has been widely used to estimate the cooperativity length at the glass transition in different glass-forming liquids, for example, in chalcogenide glasses of As-Se⁷³ and glassy polymers,⁷⁴⁻⁷⁷ as well as in the case of small molecules or polymers confined in nanogeometries^{70,71} and also multilayered polymer systems.³³ All of the parameters used to estimate N_α from eq 5 have been extracted from MT-DSC and DRS experiments (for details, see refs 69 and 78).

Figure 8 shows the evolution of the normalized cooperativity degree as a function of layer thickness. At the micrometer scale (ML-1540), the values of N_α calculated ($N_\alpha \approx 87$ for PETg and $N_\alpha \approx 70$ for PC) are in good agreement with values observed in the literature for bulk samples.^{61,74,75} Besides, when the layer thickness decreases down to the nanometer dimension, the degree of cooperativity drastically decreases by

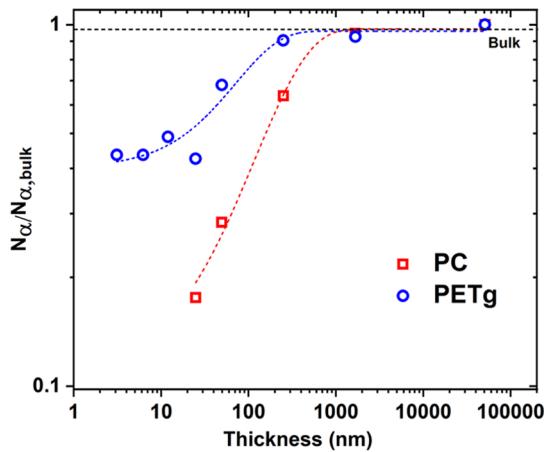


Figure 8. Evolution of the normalized cooperativity degree N_α ($N_\alpha/N_{\alpha,\text{bulk}}$) as a function of the layer thickness from MT-DSC experiments. The red and blue dashed lines are guides for the eyes.

more than $\sim 70\%$ for PC, while for PETg, this decrease is almost $\sim 40\%$. Thus, the effects of the layer thickness reduction on the cooperativity degree are very different between confining PC and confined PETg, due to different sensitivities to the confinement effect: in the case of PC, interdiffusion or structural change influences the molecular mobility at T_g ; as a result, the number of relaxing units decreases despite a small decrease in the layer thickness. This reduction can be associated with modifications of chemical and/or physical interactions between macromolecular chains and interface effects, which generally traduces confinement and/or interdiffusion effects. For confinement effects, as described previously, this can be correlated mainly with two types of interactions: the so-called finite-size effect and the one originating from the conformational changes within a particular polymeric chain.

By combining MT-DSC and DRS investigations, it is possible to follow the evolution of N_α as a function of the relaxation time or as a function of the temperature, as already shown in refs 69 79, and 80. As clearly shown in Figure 9 for

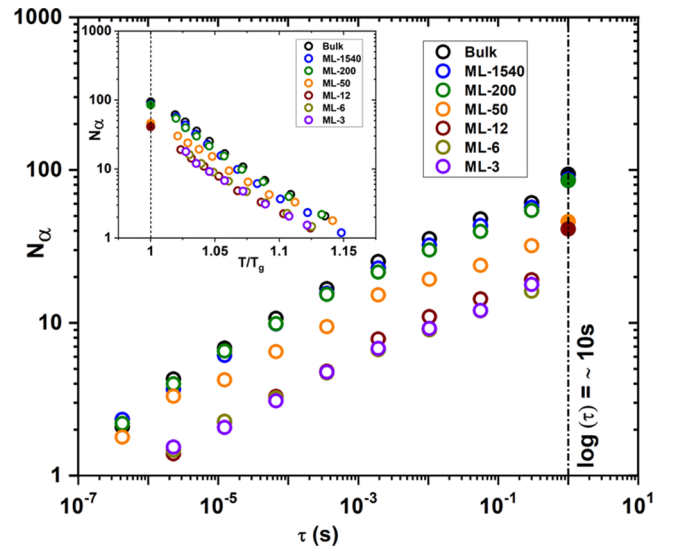


Figure 9. Evolution of the number of monomer units in a CRR N_α vs layer thickness for PETg multilayered films; hollow symbols are from DRS experiments and filled symbols from MT-DSC experiments (period = 60 s, $\tau \sim 10$ s). The inset shows N_α vs temperature normalized at T_g .

PETg, the values of N_α show similar behavior for relaxation time dependence with a shift in the N_α values on decreasing the layer thickness. A drastic decrease can also be noticed in the N_α values when the individual layer thickness becomes smaller than 50 nm. But for 12, 6, and 3 nm layer thicknesses, there is no significant change in the N_α values. The inset of Figure 9 shows the N_α evolution as a function of temperature normalized at T_g . As expected, whatever the layer thickness, the N_α values increase as the temperature decreases. However, a narrow dispersion of N_α values supports the fact that in the case of PETg the geometric confinement does not affect strongly the relaxation dynamics compared to PC.

To understand the modifications of the segmental dynamics of PETg and PC induced by the multilayering process, it is necessary to analyze the variations of molecular mobility parameters comparatively, T_g , fragility index (m), and N_α without layer thickness as a focusing parameter. From this

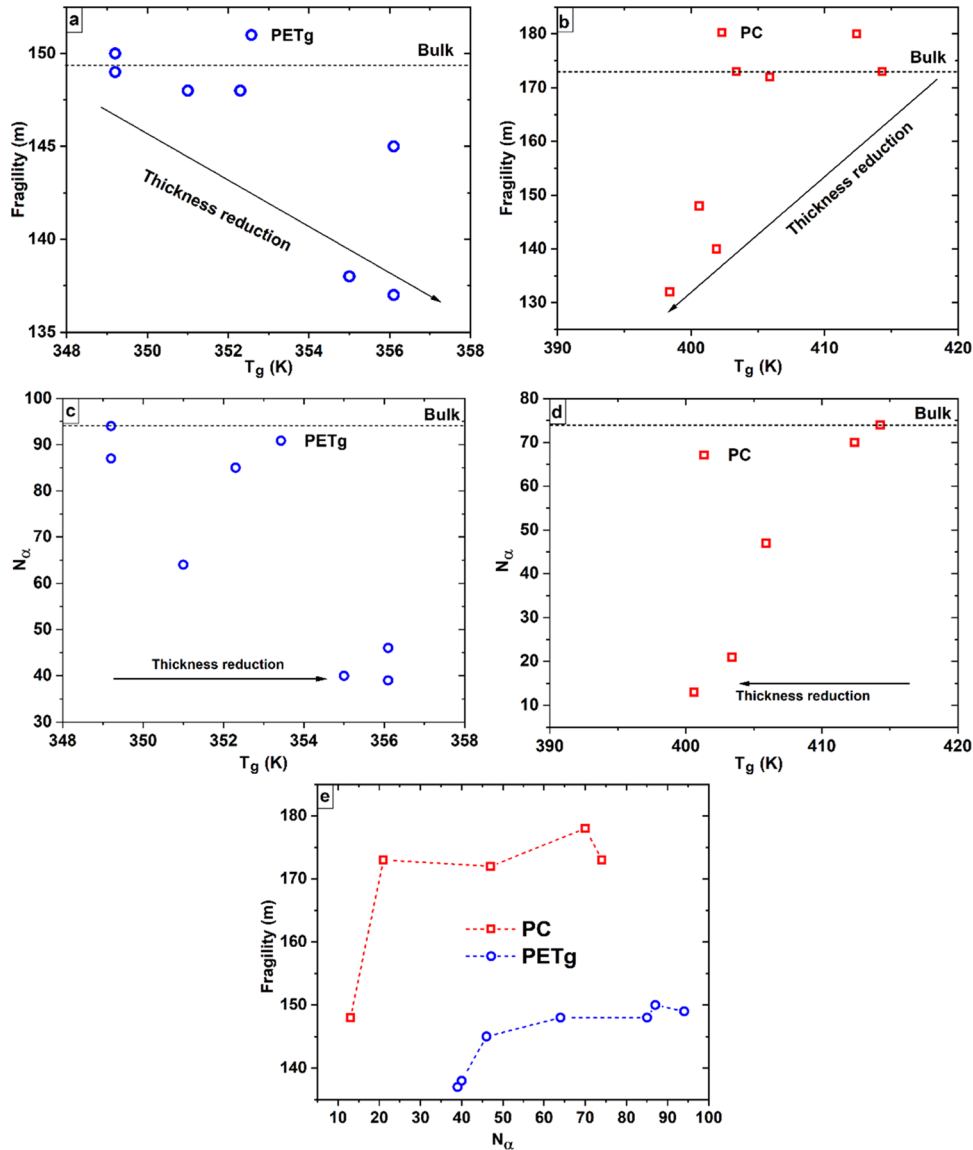


Figure 10. Fragility index (m) vs T_g for (a) PETg and (b) PC. N_α vs T_g for (c) PETg and (d) PC. (e) Fragility index (m) vs N_α for PETg and PC.

perspective, as presented in Figure 10, some significant differences appear between PETg and PC on the combined variations of these parameters at the glass transition, first of all, due to the increase of T_g for the “hard-confined” polymer (PETg) and to the decrease of T_g for the “free-confined” polymer (PC). Variations of fragility as a function of T_g (Figure 10a,b) exhibit for both polymers a two-regime behavior, a moderate variation of the fragility for bulky layers and a steeper variation for layers thinner than 20 nm. This observation is related to the fact that the fragility parameter is weakly impacted by the layer thickness reduction until the breaking of these layers (Figure 1). After the occurrence of the layer breakups, nanodroplets with typical dimensions of several nanometers are created. In these domains, the molecular mobility of each polymer is strongly impacted, and a strong reduction of fragility is observed.

For variations of cooperativity vs T_g , the trend for both polymers looks very similar, except for the amplitude of variation that is stronger for PC. A clear single-mode correlation (for PC) or anticorrelation (for PETg) is observed,

unlike fragility vs cooperativity two-mode correlations and anticorrelations.

Correlated variations of fragility and cooperativity are quite representative of a molecular mobility tracer. In the literature, the relation between these two parameters remains ambiguous. A general trend would suggest that these parameters are roughly correlated for a whole family of glass formers as suggested by Qin et al.⁸¹ and Ngai:⁵⁸ the higher the cooperativity, the higher the fragility. In a paper by Böhmer et al.,⁵⁹ a clear correlation is established between fragility and the stretching exponent of the Kohlrausch–Williams–Watts function (β) that can be linked to the cooperativity parameter in the mode coupling approach $n = 1 - \beta$. However, dealing with more specific cases, structural modifications of glass former may lead to quite different effects on the variations of these two parameters. In the literature, confinement effects are known to produce correlated variations of cooperativity and fragility whatever the structural modification applied to glass formers, hard confinement, the addition of nanoparticles, appearance of crystalline lamellae.³² These correlated variations can also be observed in glass-forming systems

where structural modifications impact intermolecular interactions in the glassy state, plasticization, and reduction of the molecular weight of the polymer.^{32,34,82–84}

As observed in Figure 10e, in multilayer films, both polymers present similar behavior, despite their quite different environments at T_g (hard-confined PETg and soft-confined PC). Even if the amplitude of variations is different for PETg compared to PC, similarly, two different correlated variations are associated with two different relaxation environments: one situated at high fragility and cooperativity values with a weak slope associated with the bulk progressive confinement of the polymer inside the layers, and another one with a much steeper variation, certainly related to strong confinement in nanodroplets, with a dramatic decrease of fragility. The latter may be associated with the amplification of the confinement effect with a strong reduction of intermolecular interactions between the same polymer macromolecules.

4. CONCLUSIONS

The influence of the layer thickness reduction on the glass transition temperature and relaxation dynamics of the α -process has been investigated in coextruded PC/PETg multilayered films with theoretical individual layer thicknesses down to 3 nm. However, AFM observations have shown that no continuous layers are visible for layer thicknesses inferior to 10 nm, suggesting the appearance of layer breakups. A complete picture of the relaxation dynamics requires a combination of several techniques, namely, calorimetric (MT-DSC) and dielectric relaxation spectroscopy (DRS). Calorimetric measurements revealed an opposite evolution of the glass transition temperatures: a slight increase of T_g for PETg (hard-confined PETg), and a huge decrease of T_g for PC (soft-confined PC) with respect to the bulk. As the layer thicknesses reach some nanometers, a broadening and asymmetric calorimetric signal is observed using MT-DSC, while two clearly distinct segmental relaxation modes are found using DRS. This indicates that the two polymers still exist as separate and distinct phases, suggesting the formation of a nanoblend (with very small droplets of some nanometers) rather than an interphasic material.

We found a moderate variation of fragility for bulky layers, and a steeper variation for layers thinner than 20 nm. The result is attributed to the fact that the fragility parameter is weakly impacted by the layer thickness reduction until the breaking of these layers and the formation of a nanoblend with a dramatic decrease of fragility. The effects of the layer thickness reduction on the cooperativity degree are very different between confining PC and confined PETg, due to different sensitivities to the confinement effect: in the case of PC, interdiffusion or structural change influences the molecular mobility at T_g ; as a result, the number of relaxing units decreases despite a small decrease in the layer thickness. Except for the amplitude of variation of cooperativity vs T_g , the trend for both polymers looks very similar. For both polymers, a clear single-mode correlation (for PC) or anticorrelation (for PETg) is observed, unlike fragility vs cooperativity two-mode correlations and anticorrelations.

Dielectric loss (ϵ'') vs frequency for bulk PC (black circles) and ML-1540 (blue circles) at 433 ± 0.2 K (Figure S1) (PDF)

AUTHOR INFORMATION

Corresponding Author

Laurent Delbreilh – INSA Rouen, UMR CNRS 6634, Groupe de Physique des Matériaux, Normandie Université, UNIROUEN Normandie, 76801 Saint Etienne du Rouvray, France; orcid.org/0000-0002-9322-7153; Email: laurent.delbreilh@univ-rouen.fr

Authors

Bidur Rijal – INSA Rouen, UMR CNRS 6634, Groupe de Physique des Matériaux, Normandie Université, UNIROUEN Normandie, 76801 Saint Etienne du Rouvray, France

Cyrille Sollogoub – Laboratoire PIMM, Arts et Metiers Institute of Technology, CNRS, CNAM, HESAM Université, 75013 Paris, France; orcid.org/0000-0003-2204-3696

Eric Baer – Department of Macromolecular Science, Case Western Reserve University, Cleveland, Ohio 44106, United States; orcid.org/0000-0001-5656-2668

Allisson Saiter-Fourcin – INSA Rouen, UMR CNRS 6634, Groupe de Physique des Matériaux, Normandie Université, UNIROUEN Normandie, 76801 Saint Etienne du Rouvray, France; orcid.org/0000-0001-9275-6865

Complete contact information is available at:

<https://pubs.acs.org/10.1021/acs.macromol.2c00691>

Notes

The authors declare no competing financial interest.

ACKNOWLEDGMENTS

The authors are grateful for the financial support from the French Ministry for Higher Education and Research. Daniele Prevosto is gratefully acknowledged for fruitful discussions and his help with DRS data analysis.

REFERENCES

- (1) Bäumchen, O.; McGraw, J. D.; Forrest, J. A.; Dalnoki-Veress, K. Reduced Glass Transition Temperatures in Thin Polymer Films: Surface Effect or Artifact? *Phys. Rev. Lett.* **2012**, *109*, No. 055701.
- (2) Pazmiño Betancourt, B. A.; Douglas, J. F.; Starr, F. W. Fragility and Cooperative Motion in a Glass-Forming Polymer–Nanoparticle Composite. *Soft Matter* **2013**, *9*, 241–254.
- (3) Madkour, S.; Yin, H.; Füllbrandt, M.; Schönhals, A. Calorimetric Evidence for a Mobile Surface Layer in Ultrathin Polymeric Films: Poly(2-Vinyl Pyridine). *Soft Matter* **2015**, *11*, 7942–7952.
- (4) Chen, Z.; Sepúlveda, A.; Ediger, M. D.; Richert, R. Dynamics of Glass-Forming Liquids. XVI. Observation of Ultrastable Glass Transformation via Dielectric Spectroscopy. *J. Chem. Phys.* **2013**, *138*, No. 12A519.
- (5) Bernazzani, P.; Sanchez, R. F.; Woodward, M.; Williams, S. Determination of the Glass Transition Temperature of Thin Unsupported Polystyrene Films Using Interference Fringes. *Thin Solid Films* **2008**, *516*, 7947–7951.
- (6) Erber, M.; Khalyavina, A.; Eichhorn, K.-J.; Voit, B. I. Variations in the Glass Transition Temperature of Polyester with Special Architectures Confined in Thin Films. *Polymer* **2010**, *51*, 129–135.
- (7) Wübbenhorst, M.; Kasina, A.; Capponi, S.; Vanroy, B.; Napolitano, S. Ultrathin Polymer Films by Single Molecule Deposition. *J. Non-Cryst. Solids* **2015**, *407*, 270–276.

- (8) Priestley, R. D.; Broadbelt, L. J.; Torkelson, J. M.; Fukao, K. Glass Transition and α -Relaxation Dynamics of Thin Films of Labeled Polystyrene. *Phys. Rev. E* **2007**, *75*, No. 061806.
- (9) Hayashi, T.; Fukao, K. Segmental and Local Dynamics of Stacked Thin Films of Poly(Methyl Methacrylate). *Phys. Rev. E* **2014**, *89*, No. 022602.
- (10) Inoue, R.; Kanaya, T.; Yamada, T.; Shibata, K.; Fukao, K. Experimental Investigation of the Glass Transition of Polystyrene Thin Films in a Broad Frequency Range. *Phys. Rev. E* **2018**, *97*, No. 012501.
- (11) Jackson, C. L.; McKenna, G. B. The Glass Transition of Organic Liquids Confined to Small Pores. *J. Non-Cryst. Solids* **1991**, *131–133*, 221–224.
- (12) Liu, T.; Siegel, R. W.; Ozisik, R. The Effect of Confinement in Nanoporous Polymers on the Glass Transition Temperature. *Polymer* **2010**, *51*, 540–546.
- (13) Tsuruta, H.; Fujii, Y.; Kai, N.; Kataoka, H.; Ishizone, T.; Doi, M.; Morita, H.; Tanaka, K. Local Conformation and Relaxation of Polystyrene at Substrate Interface. *Macromolecules* **2012**, *45*, 4643–4649.
- (14) Keddie, J. L.; Jones, R. A. L.; Cory, R. A. Size-Dependent Depression of the Glass Transition Temperature in Polymer Films. *Europhys. Lett.* **1994**, *27*, 59–64.
- (15) Beiner, M.; Huth, H. Nanophase Separation and Hindered Glass Transition in Side-Chain Polymers. *Nat. Mater.* **2003**, *2*, 595–599.
- (16) Bansal, A.; Yang, H.; Li, C.; Cho, K.; Benicewicz, B. C.; Kumar, S. K.; Schadler, L. S. Quantitative Equivalence between Polymer Nanocomposites and Thin Polymer Films. *Nat. Mater.* **2005**, *4*, 693–698.
- (17) Schönhals, A.; Goering, H.; Schick, C.; Frick, B.; Zorn, R. Glassy Dynamics of Polymers Confined to Nanoporous Glasses Revealed by Relaxational and Scattering Experiments. *Eur. Phys. J. E* **2003**, *12*, 173–178.
- (18) Füllbrandt, M.; Purohit, P. J.; Schönhals, A. Combined FTIR and Dielectric Investigation of Poly(Vinyl Acetate) Adsorbed on Silica Particles. *Macromolecules* **2013**, *46*, 4626–4632.
- (19) Napolitano, S.; Wübberhorst, M. Dielectric Signature of a Dead Layer in Ultrathin Films of a Nonpolar Polymer. *J. Phys. Chem. B* **2007**, *111*, 9197–9199.
- (20) Forrest, J. A.; Dalnoki-Veress, K.; Dutcher, J. R. Interface and Chain Confinement Effects on the Glass Transition Temperature of Thin Polymer Films. *Phys. Rev. E* **1997**, *56*, 5705–5716.
- (21) Peter, S.; Napolitano, S.; Meyer, H.; Wübberhorst, M.; Baschnagel, J. Modeling Dielectric Relaxation in Polymer Glass Simulations: Dynamics in the Bulk and in Supported Polymer Films. *Macromolecules* **2008**, *41*, 7729–7743.
- (22) Rotella, C.; Napolitano, S.; De Cremer, L.; Koeckelberghs, G.; Wübberhorst, M. Distribution of Segmental Mobility in Ultrathin Polymer Films. *Macromolecules* **2010**, *43*, 8686–8691.
- (23) Yang, Z.; Fujii, Y.; Lee, F. K.; Lam, C.-H.; Tsui, O. K. C. Glass Transition Dynamics and Surface Layer Mobility in Unentangled Polystyrene Films. *Science* **2010**, *328*, 1676–1679.
- (24) Roth, C. B.; Torkelson, J. M. Selectively Probing the Glass Transition Temperature in Multilayer Polymer Films: Equivalence of Block Copolymers and Multilayer Films of Different Homopolymers. *Macromolecules* **2007**, *40*, 3328–3336.
- (25) Xia, W.; Mishra, S.; Keten, S. Substrate vs. Free Surface: Competing Effects on the Glass Transition of Polymer Thin Films. *Polymer* **2013**, *54*, 5942–5951.
- (26) Keddie, J. L.; Jones, R. A. L.; Cory, R. A. Interface and Surface Effects on the Glass-Transition Temperature in Thin Polymer Films. *Faraday Discuss.* **1994**, *98*, 219–230.
- (27) Li, Z.; Olah, A.; Baer, E. Micro- and Nano-Layered Processing of New Polymeric Systems. *Prog. Polym. Sci.* **2020**, *102*, No. 101210.
- (28) Langhe, D. S.; Murphy, T. M.; Shaver, A.; LaPorte, C.; Freeman, B. D.; Paul, D. R.; Baer, E. Structural Relaxation of Polystyrene in Nanolayer Confinement. *Polymer* **2012**, *53*, 1925–1931.
- (29) Monnier, X.; Fernandes Nassar, S.; Domenek, S.; Guinault, A.; Sollogoub, C.; Dargent, E.; Delpouve, N. Reduced Physical Aging Rates of Poly(lactide) in Polystyrene/Poly(lactide) Multilayer Films from Fast Scanning Calorimetry. *Polymer* **2018**, *150*, 1–9.
- (30) Casalini, R.; Zhu, L.; Baer, E.; Roland, C. M. Segmental Dynamics and the Correlation Length in Nanoconfined PMMA. *Polymer* **2016**, *88*, 133–136.
- (31) Fernandes Nassar, S.; Delpouve, N.; Sollogoub, C.; Guinault, A.; Stoclet, G.; Régner, G.; Domenek, S. Impact of Nanoconfinement on Poly(lactide) Crystallization and Gas Barrier Properties. *ACS Appl. Mater. Interfaces* **2020**, *12*, 9953–9965.
- (32) Nassar, S. F.; Domenek, S.; Guinault, A.; Stoclet, G.; Delpouve, N.; Sollogoub, C. Structural and Dynamic Heterogeneity in the Amorphous Phase of Poly(l,l-Lactide) Confined at the Nanoscale by the Coextrusion Process. *Macromolecules* **2018**, *51*, 128–136.
- (33) Arabeche, K.; Delbreilh, L.; Adhikari, R.; Michler, G. H.; Hiltner, A.; Baer, E.; Saiter, J.-M. Study of the Cooperativity at the Glass Transition Temperature in PC/PMMA Multilayered Films: Influence of Thickness Reduction from Macro- to Nanoscale. *Polymer* **2012**, *53*, 1355–1361.
- (34) Arabeche, K.; Delbreilh, L.; Saiter, J.-M.; Michler, G. H.; Adhikari, R.; Baer, E. Fragility and Molecular Mobility in Micro- and Nano-Layered PC/PMMA Films. *Polymer* **2014**, *55*, 1546–1551.
- (35) Flores, A.; Arribas, C.; Fauth, F.; Khariwala, D.; Hiltner, A.; Baer, E.; Baltá-Calleja, F. J.; Ania, F. Finite Size Effects in Multilayered Polymer Systems: Development of PET Lamellae under Physical Confinement. *Polymer* **2010**, *51*, 4530–4539.
- (36) Walczak, M.; Ciesielski, W.; Galeski, A.; Potrzebowski, M. J.; Regnier, G.; Hiltner, R.; Baer, E. Structure and molecular dynamics of multilayered polycarbonate/polystyrene films. *J. Appl. Polym. Sci.* **2012**, *125*, 4267–4274.
- (37) Liu, R. Y. F.; Bernal-Lara, T. E.; Hiltner, A.; Baer, E. Polymer Interphase Materials by Forced Assembly. *Macromolecules* **2005**, *38*, 4819–4827.
- (38) Liu, R. Y. F.; Jin, Y.; Hiltner, A.; Baer, E. Probing Nanoscale Polymer Interactions by Forced-Assembly. *Macromol. Rapid Commun.* **2003**, *24*, 943–948.
- (39) Liu, R. Y. F.; Ranade, A. P.; Wang, H. P.; Bernal-Lara, T. E.; Hiltner, A.; Baer, E. Forced Assembly of Polymer Nanolayers Thinner Than the Interphase. *Macromolecules* **2005**, *38*, 10721–10727.
- (40) *Modulated Temperature Differential Scanning Calorimetry (Hot Topics in Thermal Analysis and Calorimetry)*; Reading, M.; Hourston, D. J.; Simon, J., Eds.; Springer: Dordrecht, The Netherlands, 2006; Vol. 6.
- (41) Boller, A.; Schick, C.; Wunderlich, B. Modulated Differential Scanning Calorimetry in the Glass Transition Region. *Thermochim. Acta* **1995**, *266*, 97–111.
- (42) Arabeche, K.; Delbreilh, L.; Baer, E. Physical Aging of Multilayer Polymer Films—Influence of Layer Thickness on Enthalpy Relaxation Process, Effect of Confinement. *J. Polym. Res.* **2021**, *28*, No. 431.
- (43) Bironeau, A.; Dirrenberger, J.; Sollogoub, C.; Miquelard-Garnier, G.; Roland, S. Evaluation of morphological representative sample sizes for nanolayered polymer blends. *J. Microsc.* **2016**, *264*, 48–58.
- (44) Bironeau, A.; Salez, T.; Miquelard-Garnier, G.; Sollogoub, C. Existence of a Critical Layer Thickness in PS/PMMA Nanolayered Films. *Macromolecules* **2017**, *50*, 4064–4073.
- (45) Feng, J.; Zhang, Z.; Bironeau, A.; Guinault, A.; Miquelard-Garnier, G.; Sollogoub, C.; Olah, A.; Baer, E. Breakup Behavior of Nanolayers in Polymeric Multilayer Systems — Creation of Nanosheets and Nanodroplets. *Polymer* **2018**, *143*, 19–27.
- (46) Scholtyssek, S.; Adhikari, R.; Seydewitz, V.; Michler, G. H.; Baer, E.; Hiltner, A. Evaluation of Morphology and Deformation Micromechanisms in Multilayered PP/PS Films: An Electron Microscopy Study. *Macromol. Symp.* **2010**, *294*, 33–44.
- (47) Haley, J. C.; Lodge, T. P. Dynamics of a Poly(Ethylene Oxide) Tracer in a Poly(Methyl Methacrylate) Matrix: Remarkable

- Decoupling of Local and Global Motions. *J. Chem. Phys.* **2005**, *122*, No. 234914.
- (48) He, Y.; Lutz, T. R.; Ediger, M. D. Segmental and Terminal Dynamics in Miscible Polymer Mixtures: Tests of the Lodge–McLeish Model. *J. Chem. Phys.* **2003**, *119*, 9956–9965.
- (49) Havriliak, S.; Negami, S. A Complex Plane Representation of Dielectric and Mechanical Relaxation Processes in Some Polymers. *Polymer* **1967**, *8*, 161–210.
- (50) Vogel, H. The Law of the Relation between the Viscosity of Liquids and the Temperature. *Phys. Z* **1921**, *22*, 645–646.
- (51) Fulcher, G. S. Analysis of Recent Measurements of the Viscosity of Glasses. *J. Am. Ceram. Soc.* **1925**, *8*, 339–355.
- (52) Tammann, G.; Hesse, W. Die Abhängigkeit der Viscosität von der Temperatur bei unterkühlten Flüssigkeiten. *Z. Anorg. Allg. Chem.* **1926**, *156*, 245–257.
- (53) Delbreilh, L.; Negahban, M.; Benzohra, M.; Lacabanne, C.; Saiter, J. M. Glass Transition Investigated by a Combined Protocol Using Thermostimulated Depolarization Currents and Differential Scanning Calorimetry. *J. Therm. Anal. Calorim.* **2009**, *96*, 865–871.
- (54) Xie, S.-J.; Qian, H.-J.; Lu, Z.-Y. Hard and Soft Confinement Effects on the Glass Transition of Polymers Confined to Nanopores. *Polymer* **2015**, *56*, 545–552.
- (55) Baglay, R. R.; Roth, C. B. Local Glass Transition Temperature $T_g(z)$ of Polystyrene next to Different Polymers: Hard vs. Soft Confinement. *J. Chem. Phys.* **2017**, *146*, No. 203307.
- (56) Angell, C. A. Spectroscopy Simulation and Scattering, and the Medium Range Order Problem in Glass. *J. Non-Cryst. Solids* **1985**, *73*, 1–17.
- (57) Angell, C. A. Formation of Glasses from Liquids and Biopolymers. *Science* **1995**, *267*, 1924–1935.
- (58) Ngai, K. L.; Wright, G. B. *Relaxations in Complex Systems*, Technical Report; Naval Research Laboratory: Washington DC, 1985; p 353.
- (59) Böhmer, R.; Ngai, K. L.; Angell, C. A.; Plazek, D. J. Nonexponential Relaxations in Strong and Fragile Glass Formers. *J. Chem. Phys.* **1993**, *99*, 4201–4209.
- (60) Evans, C. M.; Deng, H.; Jager, W. F.; Torkelson, J. M. Fragility Is a Key Parameter in Determining the Magnitude of T_g -Confinement Effects in Polymer Films. *Macromolecules* **2013**, *46*, 6091–6103.
- (61) Marvin, M. D.; Lang, R. J.; Simmons, D. S. Nanoconfinement Effects on the Fragility of Glass Formation of a Model Freestanding Polymer Film. *Soft Matter* **2014**, *10*, 3166–3170.
- (62) Dudowicz, J.; Freed, K. F.; Douglas, J. F. Fragility of Glass-Forming Polymer Liquids. *J. Phys. Chem. B* **2005**, *109*, 21350–21356.
- (63) Lan, T.; Torkelson, J. M. Fragility-Confinement Effects: Apparent Universality as a Function of Scaled Thickness in Films of Freely Deposited, Linear Polymer and Its Absence in Densely Grafted Brushes. *Macromolecules* **2016**, *49*, 1331–1343.
- (64) Cheng, W.; Gomopoulos, N.; Fytas, G.; Gorishnyy, T.; Walsh, J.; Thomas, E. L.; Hiltner, A.; Baer, E. Phonon Dispersion and Nanomechanical Properties of Periodic 1D Multilayer Polymer Films. *Nano Lett.* **2008**, *8*, 1423–1428.
- (65) Gao, S.; Koh, Y. P.; Simon, S. L. Calorimetric Glass Transition of Single Polystyrene Ultrathin Films. *Macromolecules* **2013**, *46*, 562–570.
- (66) Shamim, N.; Koh, Y. P.; Simon, S. L.; McKenna, G. B. Glass Transition Temperature of Thin Polycarbonate Films Measured by Flash Differential Scanning Calorimetry. *J. Polym. Sci., Part B: Polym. Phys.* **2014**, *52*, 1462–1468.
- (67) Kunal, K.; Robertson, C. G.; Pawlus, S.; Hahn, S. F.; Sokolov, A. P. Role of Chemical Structure in Fragility of Polymers: A Qualitative Picture. *Macromolecules* **2008**, *41*, 7232–7238.
- (68) Hong, L.; Gujrati, P. D.; Novikov, V. N.; Sokolov, A. P. Molecular Cooperativity in the Dynamics of Glass-Forming Systems: A New Insight. *J. Chem. Phys.* **2009**, *131*, No. 194511.
- (69) Rijal, B.; Delbreilh, L.; Saiter, A. Dynamic Heterogeneity and Cooperative Length Scale at Dynamic Glass Transition in Glass Forming Liquids. *Macromolecules* **2015**, *48*, 8219–8231.
- (70) Adam, G.; Gibbs, J. H. On the Temperature Dependence of Cooperative Relaxation Properties in Glass-Forming Liquids. *J. Chem. Phys.* **1965**, *43*, 139–146.
- (71) Donth, E. The Size of Cooperatively Rearranging Regions at the Glass Transition. *J. Non-Cryst. Solids* **1982**, *53*, 325–330.
- (72) Donth, E.-J. *The Glass Transition: Relaxation Dynamics in Liquids and Disordered Materials*; Springer Science & Business Media, 2001.
- (73) Saiter, A.; Saiter, J.-M.; Golovchak, R.; Shpotyuk, M.; Shpotyuk, O. Cooperative Rearranging Region Size and Free Volume in As–Se Glasses. *J. Phys. Condens. Matter* **2009**, *21*, No. 075105.
- (74) Lixon, C.; Delpouve, N.; Saiter, A.; Dargent, E.; Grohens, Y. Evidence of Cooperative Rearranging Region Size Anisotropy for Drawn PET. *Eur. Polym. J.* **2008**, *44*, 3377–3384.
- (75) Kahouli, A.; Sylvestre, A.; Jomni, F.; Yangui, B. Evaluation of Activation Parameters of Molecular Mobility of Parylene C Using Differential Scanning Calorimetry, Dielectric Spectroscopy, and Thermally Stimulated Depolarization Currents. *J. Phys. Chem. A* **2014**, *118*, 1320–1330.
- (76) Saiter, A.; Couderc, H.; Grenet, J. Characterisation of Structural Relaxation Phenomena in Polymeric Materials from Thermal Analysis Investigations. *J. Therm. Anal. Calorim.* **2007**, *88*, 483–488.
- (77) Puente, J. A. S.; Rijal, B.; Delbreilh, L.; Fatyeyeva, K.; Saiter, A.; Dargent, E. Segmental Mobility and Glass Transition of Poly-(Ethylene-Vinyl Acetate) Copolymers: Is There a Continuum in the Dynamic Glass Transitions from PVAc to PE? *Polymer* **2015**, *76*, 213–219.
- (78) Rijal, B.; Delbreilh, L.; Saiter, J.-M.; Schönhals, A.; Saiter, A. Quasi-Isothermal and Heat–Cool Protocols from MT-DSC. *J. Therm. Anal. Calorim.* **2015**, *121*, 381–388.
- (79) Saiter, A.; Delbreilh, L.; Couderc, H.; Arabeche, K.; Schönhals, A.; Saiter, J.-M. Temperature Dependence of the Characteristic Length Scale for Glassy Dynamics: Combination of Dielectric and Specific Heat Spectroscopy. *Phys. Rev. E* **2010**, *81*, No. 041805.
- (80) Rijal, B.; Soto Puente, J. A.; Atawa, B.; Delbreilh, L.; Fatyeyeva, K.; Saiter, A.; Dargent, E. Correlated and Cooperative Motions in Segmental Relaxation: Influence of Constitutive Unit Weight and Intermolecular Interactions. *Phys. Rev. E* **2016**, *94*, No. 062502.
- (81) Qin, Q.; McKenna, G. B. Correlation between Dynamic Fragility and Glass Transition Temperature for Different Classes of Glass Forming Liquids. *J. Non-Cryst. Solids* **2006**, *352*, 2977–2985.
- (82) Zhang, C.; Guo, Y.; Priestley, R. D. Characteristic Length of the Glass Transition in Isochorically Confined Polymer Glasses. *ACS Macro Lett.* **2014**, *3*, 501–505.
- (83) Saiter, A.; Prevosto, D.; Passaglia, E.; Couderc, H.; Delbreilh, L.; Saiter, J. M. Cooperativity Length Scale in Nanocomposites: Interfacial and Confinement Effects. *Phys. Rev. E* **2013**, *88*, No. 042605.
- (84) Schick, C.; Donth, E. Characteristic Length of Glass Transition: Experimental Evidence. *Phys. Scr.* **1991**, *43*, 423–429.